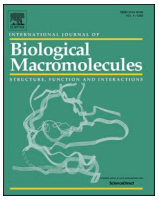
International Journal of Biological Macromolecules 282 (2024) 137218



Contents lists available at ScienceDirect

International Journal of Biological Macromolecules

journal homepage: www.elsevier.com/locate/ijbiomac





Protective fibrous structures based on cellulose fibers functionalized with metal oxide nanoparticles by electrospinning and electrospray deposition

Joana C. Araújo [a,*], Pedro M. Silva [b], Miguel A. Cerqueira [b], Pilar Teixeira [c,d], Vânia Tira-Picos [e], Pedro Neto [e], Olívia Salomé G.P. Soares [f,g], Cátia L. Graça [f,g], Raul Fangueiro [a,h], Diana P. Ferreira [a]

[a] Centre for Textile Science and Technology (2C2T), University of Minho, Guimarães 4800, Portugal
[b] International Iberian Nanotechnology Laboratory, Av. Mestre José Veiga s/n, Braga 4715-330, Portugal
[c] CEB - Centre of Biological Engineering, University of Minho, Braga 4710-057, Portugal
[d] LABBELS –Associate Laboratory, Guimarães, Portugal
[e] Unidade Militar Laboratorial de Defesa Biológica e Química, Lisboa, Portugal
[f] Laboratory of Separation and Reaction Engineering-Laboratory of Catalysis and Materials (LSRE-LCM), Faculty of Engineering, University of Porto, Rua Dr. Roberto Frias, Porto 4200-465, Portugal
[g] ALiCE—Associate Laboratory in Chemical Engineering, Faculty of Engineering, University of Porto, Rua Dr. Roberto Frias, Porto 4200-465, Portugal
[h] Department of Textile Engineering, University of Minho, Guimarães, Portugal

ARTICLE INFO

Keywords:
Metal oxide nanoparticles
Natural fibers
Electrospinning
Electrospray deposition
Antibacterial activity
DMMP degradation

ABSTRACT

This work aims to develop a bio-based fibrous material that is able to adsorb and degrade chemical and biological hazardous agents. Thus, cellulosic fabrics (flax) were functionalized with chitosan (CS) and poly(ethylene oxide) (PEO) electrospun nanofibers doped with titanium dioxide (TiO_2) and cerium dioxide (CeO_2) nanoparticles (NPs). The electrospray deposition of these NPs was also tested. The TiO_2 NPs were synthesized using a very straightforward precipitation method. The successful synthesis was confirmed by Scanning Transmission Electron Microscopy (STEM) and Attenuated Total Reflectance-Fourier-Transform Infrared Spectroscopy (ATR-FTIR). The functionalization of the fabrics with the NPs and the nanofibers doped with NPs was proved by Field Emission Scanning Electron Microscopy (FESEM), ATR-FTIR, and Ground-State Diffuse Reflectance (GSDR). The developed samples presented antibacterial activity against *Staphylococcus aureus* (ATCC 6538) and *Escherichia coli* (ATCC 434), reaching values of 99.97 and 100.0 %, respectively. The degradation of methylene blue (MB) and dimethyl methylphosphonate (DMMP) was evaluated. The best samples were able to decompose 97.82 % of DMMP. The wash durability of the nanocoating was also tested. The developed fibrous structures show great potential for personal protection applications.

1. Introduction

The development of technologies to protect humans from harmful threats is becoming increasingly important, not only because of the recent pandemic but also due to rising concerns over chemical and biological warfare. The scientific community has been dedicating substantial efforts to developing textiles with specific properties to protect against various environmental factors, hazards, or specific threats. This can be accomplished by the incorporation of NPs with known functionalities like easy/self-cleaning, decomposition of chemical agents, antimicrobial activity, UV protection, and monitoring/sensing behavior on textiles [1]. Metal oxides, especially TiO_2 NPs, present excellent properties and exceptional photocatalytic activity, being able to degrade hazardous chemical agents [1]. TiO_2 NPs are valuable semiconductors in the field of solar cells, environmental clean-up, and photocatalysis. Additionally, they have attracted special interest due to their low cost, stability, and recyclability, among others. Therefore, TiO_2 photocatalysts have been increasingly used in areas regarding human health and energy-related sciences [2]. CeO_2 NPs have also received a lot of attention due to their large array of applications, namely in environmental remediation, photocatalytic dye degradation, biological applications, and several industrial fields [3,4]. Additionally, the

* Corresponding author.
E-mail address: joanaaraujo@det.uminho.pt (J.C. Araújo).

https://doi.org/10.1016/j.ijbiomac.2024.137218
Received 18 June 2024; Received in revised form 28 October 2024; Accepted 1 November 2024
Available online 7 November 2024
0141-8130/© 2024 The Authors. Published by Elsevier B.V. This is an open access article under the CC BY-NC-ND license (http://creativecommons.org/licenses/by-nc-nd/4.0/).

photocatalytic performance of TiO_2 can be greatly improved by the addition of CeO_2, since this combination can promote charge separation and narrow the band gap by semiconductor heterojunction, leading to a more efficient photocatalysis process [5]. Additionally, these nanomaterials present exceptional antibacterial activity performance, which is crucial for the degradation of biological agents [6–11]. Therefore, the potential degradation of harmful compounds is improved with the mixture of these two NPs.

The functionalization of textiles with NPs presents one major drawback, the poor adhesion of the nanomaterials onto the fibers' surface. Electrospinning can configure a promising strategy to address this issue and improve the anchorage of the NPs onto the fabrics. This technique has been gaining interest in the development of high-performance fibers, as it allows the production of fibers from the nano to the microscale. In addition, it is a cost-effective, simple, and versatile technique [12]. Electrospun nanofibers can be deposited directly onto a textile substrate, which will not only improve the bonding of the NPs onto the substrate but also increase the specific surface area and the filtration capacity, which results in higher adsorption of contaminants [13].

A wide range of polymers can be used to produce electrospun nanofibers, including biopolymers such as chitosan (CS), a biopolymer that is derived from chitin deacetylation and that can be found on crustacean's (shrimps, lobsters, and crabs) shells as well as in fungi and algae cell walls. CS has great properties, being widely used due to its biodegradability, biocompatibility, non-toxicity, and antimicrobial activity, which is of great importance for the protection against biological agents [14–16]. However, the electrospinnability of CS is limited, making it difficult to produce neat CS nanofibers, due to its rigid chemical structure, polycationic nature, and specific inter and intramolecular hydrogen bond interactions. Therefore, a co-spinning agent must be used, like poly(ethylene oxide) (PEO), which is also biodegradable, biocompatible, and non-toxic [14,17,18].

Another issue related to the deposition of NPs onto fabrics is the distribution of nanomaterials since they tend to agglomerate. One approach could be the deposition of the synthesized NPs by electrospray. In this technique, the solution containing the NPs passes through the needle connected to a high-voltage power supply at a constant flow rate. Then, the solution forms a Taylor cone due to the potential difference that is elongated due to the electric field being atomized into small droplets. As these droplets are highly charged, agglomeration is prevented, resulting in a more homogenous distribution of the NPs onto the fabrics [19,20].

For the development of personal protective equipment, synthetic fibers emerge as the most valuable options, such as high temperature (HT) polyamide, ultra-high molecular weight (UHMWPE), and aramid. Although the use of natural fibers in this application is not as common, they could be a viable alternative to replace synthetic ones due to their low cost, lightness, durability, abundance, biocompatibility, and biodegradability [1]. One of the oldest and most popular natural fiber is flax due to its great mechanical properties, being widely used as reinforcements in composite materials [21,22]. Additionally, incorporating flax into blends can enhance various textile characteristics, including improved dye absorption, reduced shrinkage, and shorter drying times [23]. Therefore, the use of flax fabrics and their functionalization by electrospinning and electrospraying with blends of CS, PEO, TiO_2, and CeO_2 NPs could be a suitable approach for the development of more sustainable fibrous structures that can replace or complement the already existent personal protective equipment.

Given this, the main focus of this work is the optimization and development of innovative fibrous structures able to degrade bacteria and hazardous chemical agents (methylene blue (MB) and dimethyl methylphosphonate (DMMP)). MB is usually used as a model compound for photocatalytic evaluation and DMMP is a simulant for nerve agents [24,25]. To achieve this, two distinct approaches were implemented and compared: a) the coating of flax fabrics with electrospun CS/PEO nanofibers doped with TiO_2 and CeO_2 NPs and b) the flax fabrics coated by electrospraying with TiO_2 and CeO_2 NPs. This has not yet been published in literature, as far as the authors are aware. The TiO_2 NPs were characterized by Scanning Transmission Electron Microscopy (STEM) and Attenuated Total Reflectance-Fourier-Transform Infrared Spectroscopy (ATR-FTIR), confirming their successful synthesis. The fabrics functionalized with TiO_2 and CeO_2 NPs by electrospray and electrospinning were characterized by ATR-FTIR, Ground-State Diffuse Reflectance (GSDR), Field Emission Scanning Electron Microscopy (FESEM) and Energy Dispersive X-ray Spectrometry (EDX), which confirmed the successful functionalization of the flax fabrics with the NPs, as well as their incorporation onto the electrospun nanofibers. To evaluate the potential of these materials to be used against biological and chemical threats, the antimicrobial activity against *Staphylococcus aureus* and *Escherichia coli* was evaluated as well as degradation essays using MB and DMMP (chemical agents). The washing durability of the developed samples was also tested.

2. Materials and methods

2.1. Materials

The flax fabrics used in this work, with 315 g/m^2 of fabric weight, were supplied by RCS (Braga, Portugal) and produced using 100 % flax natural yarns (Bangladesh origin). Titanium(IV) butoxide ($Ti(OBu)_4$) CS (high molecular weight, 310,000–375,000 Da) and PEO (molecular weight 900 kDa) powders were purchased from Sigma-Aldrich. Memmert UNE 800 oven was used. UV blacklight lamp (15 W) from HQ™ was utilized for photocatalytic tests. For the DMMP degradation tests, DMMP 97 % and Diethyl methylphosphonate (DEMP) 97 % from Sigma-Aldrich were used.

2.2. TiO_2 and CeO_2 nanoparticles synthesis

In order to synthetise TiO_2 NPs, 5 mL of $Ti(OBu)_4$ was slowly added (drop wise) to 8 mL of distilled water. The solution was kept under mechanical stirring at 40 °C for 30 min. A white precipitate was formed at the bottom of the beaker which was centrifugated and washed three times with water and ethanol. Then, the resulting white powder was air-dried for two days and calcinated at 150 °C for 6 h. The CeO_2 NPs used in this study were previously synthesized by precipitation of cerium nitrate as precursor followed by thermal treatment under 100 cm^3/min air flow at 450 °C for 3 h and characterized in an earlier work [26] and were employed here without further modification.

2.3. Fabrics pre-treatment

Firstly, the flax fabrics (5 cm × 5 cm) were washed with 5 % (*v*/v) of a non-ionic detergent at 80 °C for 30 min. to remove impurities (waxes, fats, etc). The fabrics were further cleaned in distilled water at 70 °C for 30 min. and dried at 100 °C for 1 h.

2.4. Electrospray deposition

The electrospray deposition of the NPs onto flax fabrics was performed using ethanolic suspensions of TiO_2 and TiO_2/CeO_2 NPs with a concentration of 0.5 % (*w/v*). The suspensions were electrosprayed on the surface of the pre-treated flax fabrics. The electrospinning equipment used was a Fluidnatek® LE-50 from Bioinicia S.L., equipped with a high-voltage power supply (0–30 kV). The syringe was coupled to a digitally controlled syringe pump (Bioinicia S.L. Valencia, Spain). A coaxial nozzle was used, being that ethanol was flowing in the outer needle (0.71 mm) to prevent the NPs suspension from drying out. The optimized electrospinning parameters that allowed the formation of a stable jet are described in Table 1.

Table 1
Processing parameters used for the deposition of TiO_2 and TiO_2/CeO_2 NPs on flax fabrics.

Processing parameters	Optimized values
Applied voltage	10 kV
Feed rate	5 mL/h
Needle-to-collector distance	150 mm
Inner needle diameter	0.60 mm
Deposition time	30 min.
Type of collector	Static
Humidity	59–65 %
Temperature	19-21 °C

2.5. Preparation CS/PEO polymeric solutions incorporated with TiO_2 NPs and CeO_2 NPs

For the synthesis of defect-free nanofibers, a CS/PEO solution with a weight ratio of 1:1 and a total polymer concentration of 2 % (*w/v*) was prepared in a 50 % (v/v) acetic acid solution. The solution was kept under mechanical stirring for 8 h and then centrifugated at 5000 rpm for 30 min. as described in [14]. A concentration of 0.5 % (*w/v*) of the previously synthesized TiO_2 NPs was added to the solution and kept under mechanical stirring overnight. For the samples with the two NPs (TiO_2 and CeO_2), 0.5 % (w/v) of each was added to the polymeric solution as referred previously.

2.6. Electrospinning process

The CS/PEO, CS/PEO-TiO_2, and the CS/PEO-TiO_2/CeO_2 solutions were electrospun in an electrospinning NF-103 equipment from MECC and deposited directly onto the pre-treated flax fabrics (Fig. 1). The optimized equipment conditions that allowed the formation of a stable jet and the production of defect-free nanofibers are described in Table 2.

2.7. Samples characterization

2.7.1. Scanning electron microscopy (SEM)

The surface of the flax fabrics functionalized with the NPs by electrospray deposition was characterized by SEM, using a FEI Quanta 650FEG. The samples were coated with a thin film (20 nm) of Gold (Au) and Palladium (Pd) before the analysis and examined at 10 kV.

The surface morphology of the flax fabrics functionalized with the NPs by electrospray deposition was observed using a scanning electron microscope (Quanta 650 FEG, FEI, USA). The samples were placed on an aluminum support using a double-side carbon conductive tape and coated with gold (Au) and Palladium (Pd) (20 nm layer) using a Leica EM ACE200.

Table 2
Processing parameters used for the production and deposition of electrospun nanofibers.

Processing parameters	Optimized values
Applied voltage	29 kV
Feed rate	4 mL/h
Needle-to-collector distance	170 mm
Needle diameter	0.41 mm
Deposition time	2 h
Head transverse speed	150 mm
Head transverse distance	50 mm/s
Type of collector	Static
Humidity	59–65 %
Temperature	19-21 °C

2.7.2. Field emission scanning electron microscopy (FESEM)

The surface of the fabrics coated with the doped nanofibers was studied by FESEM using NOVA 200 Nano SEM from FEI Company (Hillsboro, OR, USA). The samples were coated with a thin film (20 nm) Au/Pd before the analysis. The images were taken in topographic mode with an accelerated voltage of 10 kV.

2.7.3. Attenuated total reflectance-Fourier transform infrared spectroscopy (ATR-FTIR)

The chemical composition of the synthesized NPs and the functionalized flax fabrics was studied by ATR-FTIR analysis using an IRAffinity-1S, SHIMADZU equipment (Kyoto, Japan). The spectra were obtained in transmittance mode, With a spectral resolution of 8 cm^{-1}, for 45 scans in the range of 400 to 4000 cm^{-1}. The samples were analysed in 3 different places and an average was done from the 3 analyses, to ensure the homogeneity of the analysis.

2.7.4. Scanning transmission electron microscopy (STEM)

The morphology of the synthesized TiO_2 NPs was studied by STEM using a NOVA 200 Nano SEM from FEI Company (Hillsboro, OR, USA) with a scanning transmitted electron microscopy detector. The STEM

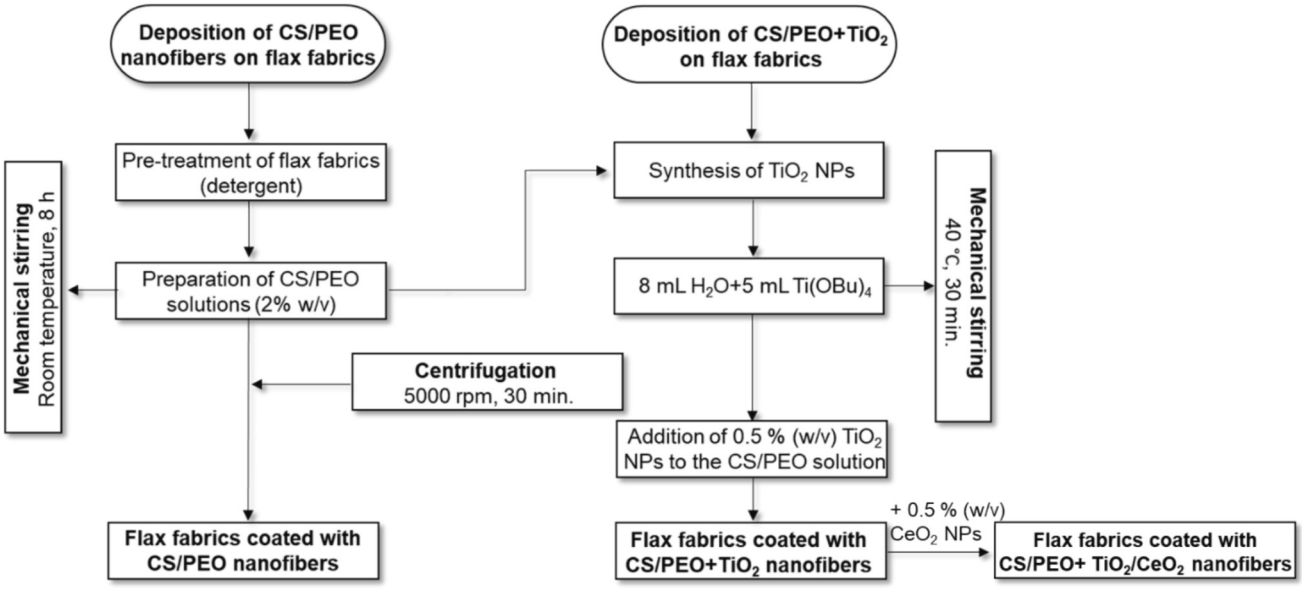


Fig. 1. Schematic flow chart of the electrospinning and deposition of CS/PEO and CS/PEO + TiO_2 NPs onto the surface of flax fabrics.

grids were dipped into an ethanol suspension containing the NPs and then dried.

2.7.5. Ground-state diffuse reflectance (GSDR)

The fabrics coated with the functionalized nanofibers were analysed by GSDR. The reflectance and transmittance spectra were recorded using a Spectrophometer UV-2600 (Schimadzu) with the ISR_2600 Plus detector. The calibration was made using as blank barium sulphate (full reflectance).

Five spots of the samples were analysed to ensure the analysis' homogeneity. The reflectance spectra were recorded, in the 200 to 800 nm wavelength, and the remission function was calculated accordingly with the Kubelka-Munk equation:

$$\frac{K}{S} = \frac{[(1-R)]^2}{2 \times R}$$

where, K represents the absorption coefficient, S the dispersion coefficient and R the reflectance [27].

2.8. Properties evaluation

2.8.1. Antibacterial activity tests

The antibacterial activity of the flax fabrics functionalized with TiO_2 and CeO_2 NPs by the electrospraying deposition method as well as of the flax fabrics with the nanofibers produced by electrospinning process was evaluated through the Absorption method from the Japanese industrial standard (JIS L 1902: 2002, "Testing method for antibacterial activity of textiles"). *Staphylococcus aureus* ATCC 6538 (Gram-positive bacteria) and *Escherichia coli* ATCC 434 (Gram-negative bacteria) were the bacteria tested. Briefly, inocula of the two bacteria were prepared in 20.0 ± 0.1 mL of TSB (Tryptic Soy Broth, Merck) and incubated for a period of 18 to 24 h at 37 ± 1 °C under agitation (120 rpm). Then, microbial concentrations were adjusted to 3×10^8 cells/mL via absorbance readings and based on a corresponding calibration curve. An aliquot of each suspension (400 μL) was added to 20 mL of TSB for *Escherichia coli* and *Staphylococcus aureus* and incubated for 3 h at 37 ± 1 °C. The microbial concentration was again measured and 3×10^5 cells/mL were obtained using a 20-fold dilution of the respective medium (in distilled water). The samples were placed in Petri dishes and 50 μL of this inoculum was added. Samples were incubated for 24 h at 37 ± 1 °C, without agitation. To release the bacterial cells from the flax samples, 5 mL of physiological saline solution (8.5 g of NaCl and 2.0 g of non-ionic surfactant Tween 20 (Sigma Chemical Co.) per litre) were added and then vortexed (5 times, 5 s each time). The number of living cells was assessed by the serial dilution plate count method. All assays were performed in triplicate and repeated, at least, in three independent assays.

The antibacterial activity (%) after 24 h incubation was calculated by the formula:

$$\text{Antibacterial activity } (\%) = [(B-A)/B] \times 100$$

where A represents the number of bacteria in the tested sample after 24 h and B the number of bacteria in the starting suspension before the addition of the sample.

2.8.2. Methylene blue degradation

MB was used as a degradation model compound to evaluate the photocatalytic activity of the TiO_2 and CeO_2 NPs electrosprayed on the flax fabrics and incorporated onto de CS/PEO nanofibers. A drop (500 μL) of a MB solution (1 g/L) was placed in the centre of the functionalized fabrics (5 cm × 5 cm). The samples were dried and kept in the dark for 30 min., in order to reach the adsorption/desorption equilibrium. Then, they were irradiated by a UV blacklight lamp for 24 h and monitored hourly by GSDR.

2.8.3. DMMP degradation

In order to study the possible degradation of DMMP, samples of flax fabrics coated with CS/PEO nanofibers doped with TiO_2 and CeO_2 NPs were tested. Initially, a calibration curve was plotted using different concentrations of DMMP and DEMP. The flax samples with 1.5 cm × 1.5 cm were placed onto a headspace (HS) vial and a standard solution of DMMP (20 μL) was dropped onto the surface of the fabric. Then, after encapsulation, the samples were kept in the dark for 10 min. to reach the adsorption-desorption equilibrium. The samples were then irradiated under a UV lamp for 0,1, 2, 3, 4, 5, 6, 18, and 24 h. The internal standard (DEMP) was added in liquid chromatography (LC) vial to the HS vial, encapsulated, incubated for 10 min. at 120 °C and analysed by gas chromatography–mass spectrometry (GC–MS). GC–MS analysis was performed in a Bruker SCION 456-GC SQ. The injector and transfer line temperatures were 215 and 290 °C, respectively, and the injection was performed in spiltless mode with a gas flow of 1.20 mL/min. Mass spectra were scanned from m/z 50–200 with an acquisition rate of 500 spectra ms^{-1}.

2.9. Wash fastness

The wash durability of the CS/PEO-TiO_2 and CS/PEO-TiO_2/CeO_2 nanocoating was evaluated using an adaptation of the standard "ISO6330-Textiles, Domestic Washing and drying, procedures for textile testing", in order to mimic the domestic washing programs. According to this standard, the agitation speed ranges between 119 and 179 rpm, for delicate and durable press parameters, respectively. Thus, the functionalized samples were placed in contact with distilled water and centrifugated at 200 rpm for 24 h, continuously. Aliquots of the washing solution (3 mL), in contact with the flax fabrics functionalized with the CS/PEO nanofibers doped with TiO_2 and TiO_2/CeO_2 NPs were withdrawn, and their absorbance was measured by UV–visible spectroscopy after 1, 2, 4, 5, 6, 7 and 24 h, to monitor the release of the NPs. The NPs' loss percentage was also calculated, to infer the quantity of NPs that were still fixed onto the fabrics, even after continuous contact with water.

2.10. Statistical tests

JASP software (JASP Team (2023), JASP Version 0.18.3) was used for all statistical analysis.

3. Results and discussion

3.1. TiO_2 NPs' synthesis

As mentioned before, for the synthesis of TiO_2 NPs, $Ti(OBu)_4$ was used as a precursor agent. The addition of $Ti(OBu)_4$ to water led to alkoxide hydrolysis and precipitation of hydrous titanium oxide [28]. At the end of the reaction, a white precipitate was formed at the bottom of the beaker and the TiO_2 NPs were separated by centrifugation and washed several times. The resulting NPs were characterized by ATR-FTIR and STEM (Fig. 2).

The ATR-FTIR spectrum of the TiO_2 NPs powder is shown in Fig. 2a. The broad absorption band at around 3300 cm^{-1} is associated with the stretching mode of H_2O molecules and hydroxyl (O—H) groups. The band peaking at around 1630 cm^{-1} may be attributed to the deformative vibration of Ti-OH stretching mode, which is probably related to water adsorbed on the NPs' surface. The last adsorption band at around 480 cm^{-1} corresponds to the Ti—O bending mode, which is characteristic of TiO_2 NPs [29–31].

STEM images from the developed TiO_2 NPs are shown in Fig. 2b. From these images, we can observe that synthesized particles seem to present a spherical morphology. It's also possible to see the formation of some agglomerates, which is characteristic of TiO_2 NPs [28]. The diameter of the NPs was measured by the analysis of the STEM images,

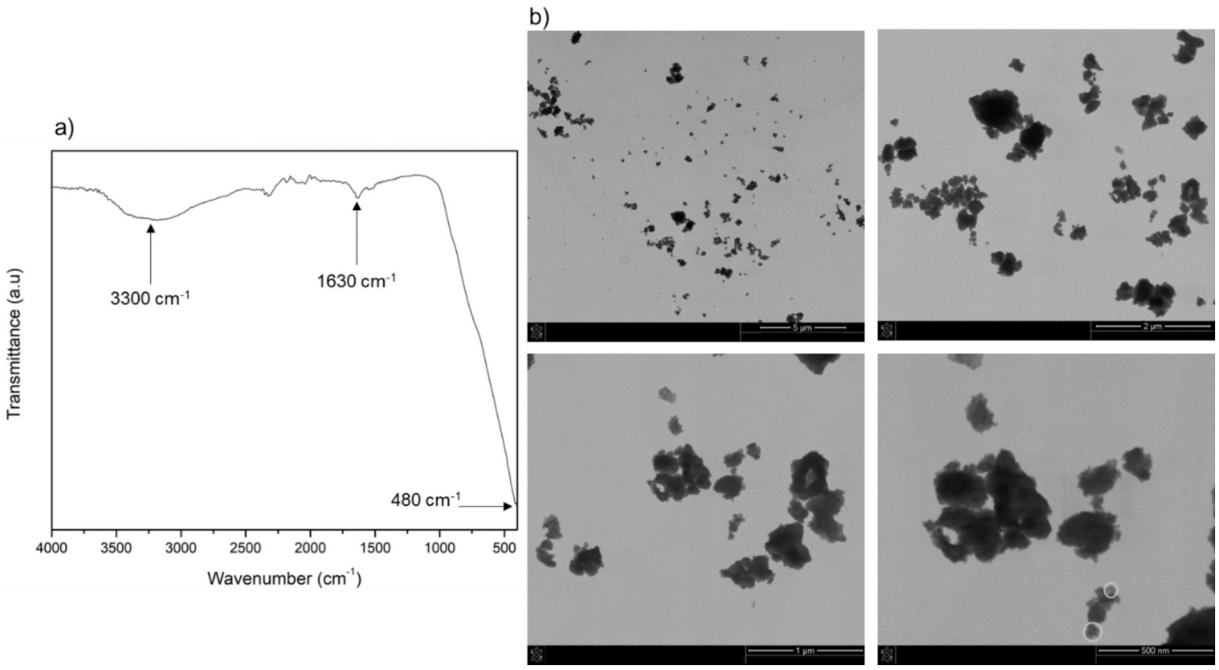


Fig. 2. TiO_2 NPs' characterization: a) ATR-FTIR spectrum and b) STEM images of the synthesized TiO_2 NPs (scale bars 5, 2, 1 μm and 500 nm).

using the *Image J* software. It was demonstrated that the NPs presented a mean diameter of 43.3 ± 25.2 nm.

From not only the analysis of the ATR-FTIR spectrum but also from the STEM images is possible to conclude that the TiO_2 NPs were successfully synthesized using a very simple precipitation method and fairly sustainable conditions, namely the use of water as solvent, low reaction times, and a low calcination temperature. This method is more straightforward compared to similar approaches for synthesizing TiO_2 NPs, involving fewer steps and reagents. It is also a fast process, utilizing materials and methods that are relatively accessible and well-established, thereby enhancing the industrial scalability of the developed synthesis. Typically, the synthesis of TiO_2 NPs involves less sustainable reagents, higher calcination temperatures, and longer reaction times [28,32,33]. Conversely, in this work, the procedure was optimized to enhance the sustainability of commonly used processes by utilizing water as a solvent and reducing both reaction times and calcination temperatures. The CeO_2 NPs were used as received [26].

3.2. Electrospray deposition of TiO_2 and CeO_2 NPs on flax fabrics

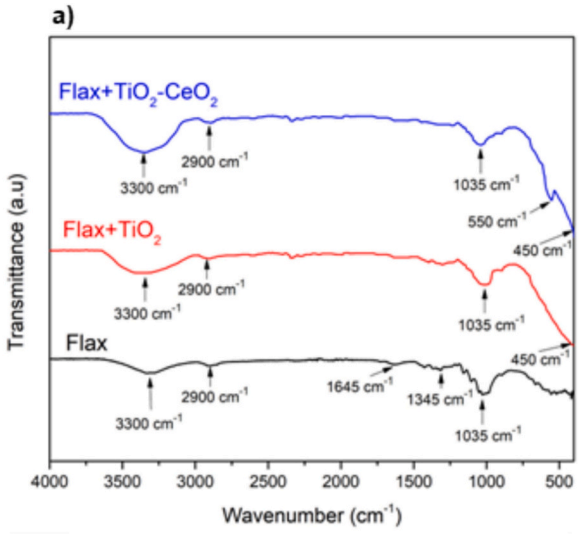
After the successful synthesis, the NPs were electrosprayed onto the fabric's surface. For this purpose, several ethanolic suspensions of NPs were optimized and were electrosprayed onto the flax fabrics surface using the parameters: concentration of 0.5 % (*w/v*) TiO_2 and TiO_2, and CeO_2 NPs, applied voltage of 10 kV, feed rate of 5 mL/h, needle-collector distance of 150 mm and deposition time of 30 min. Fig. 3 shows the characterization of the developed samples.

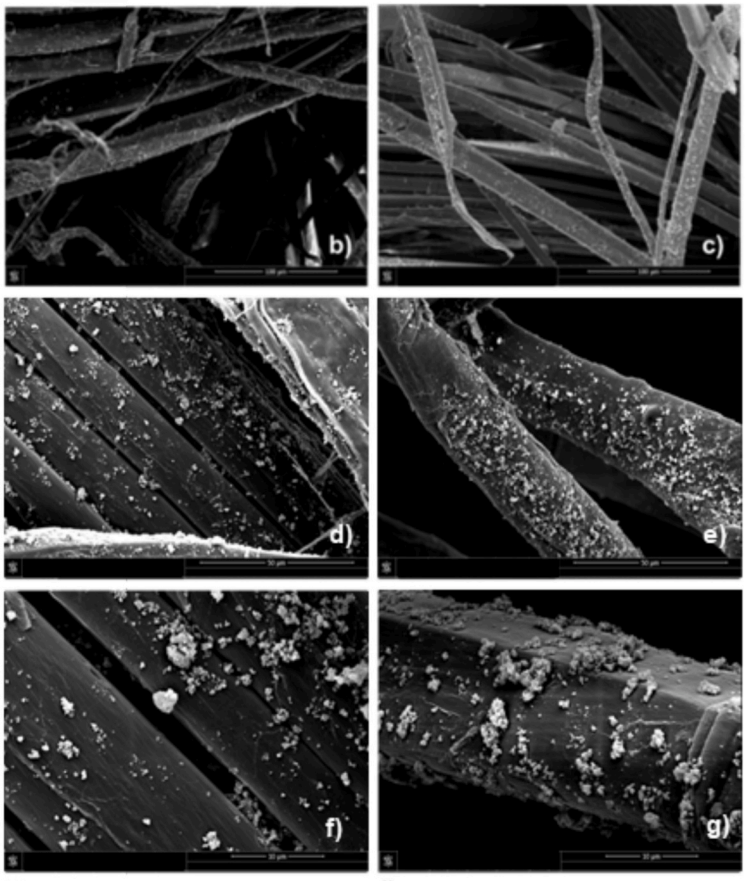
The ATR-FTIR spectra of flax fabrics, flax/TiO_2 NPs, and flax/TiO_2/CeO_2 NPs coated by electrospray deposition are presented in Fig. 3a. The spectrum of only the flax fabrics shows the characteristic peaks of natural cellulosic fibers, namely cellulose, hemicellulose, and lignin. The broad band at approximately 3300 cm^{-1} can be attributed to the hydroxyl groups from cellulose or to the presence of adsorbed water molecules. The band peaking at 2900 cm^{-1} is probably related to the asymmetric C—H stretching vibration of cellulose and hemicellulose. The band at around 1645 cm^{-1} represents C═C stretching from lignin and the band at approximately 1345 cm^{-1} to the C—H bending of the aromatic rings in cellulose polysaccharides. At 1035 cm_{-1} we can see the band of (CO) and (OH) stretching vibrations of the polysaccharide in cellulose [21,34–37]. Looking at the spectrum of the flax fabrics functionalized with the TiO_2 NPs, and comparing it to the previously analysed spectrum, it is possible to observe the appearance of a new band, peaking at around 450 cm^{-1}, which is characteristic of TiO_2 NPs, as shown in the analysis of the spectrum of Fig. 2. Finally, and by the comparison of the spectrum of the samples functionalized with only the TiO_2 NPs with the ones functionalized with TiO_2 and CeO_2 NPs, is possible to see the appearance of the band at around 550 cm^{-1} related to the Ce—O stretching vibration, which proves the successful functionalization of the flax fabrics with the two types of NPs in the study [38,39]. It's also possible to observe the increase of the intensity of the band at around 3300 cm^{-1}, which is likely associated with the stretching vibrations of the O—H bonds, which can show that there was the establishment of hydrogen bonds between the hydroxyl groups of the flax and the CeO_2 NPs [34]. Therefore, for the samples with CeO_2, the NPs seem to be more anchored to the surface of the flax fabrics.

From the SEM images of the flax fabrics functionalized with TiO_2 (Fig. 3b, d, f) and TiO_2 and CeO_2 NPs (Fig. 3c, e, g) by electrospray deposition it's possible to observe that this technique allowed a very homogeneous distribution of the NPs all over the flax fabrics surface. Both the TiO_2 but also the CeO_2 NPs are present in the fabric and few agglomerates were formed. More particles were present on the surface of the fabrics functionalized with the two NPs, as expected. Through these results, was possible to confirm that the TiO_2 and CeO_2 NPs were successfully deposited onto the surface of the flax fabrics by electrospraying.

The EDX results of the samples with TiO_2 and TiO_2 and CeO_2 NPs (Fig. 3h and i) also proved the successful functionalization of the fabrics with these nanomaterials, since the presence of titanium (Ti) and cerium (Ce) was detected. Additionally, carbon (C) and oxygen (O) were also found, which is in accordance with the anticipated results, since the substrate used in this work was a natural fiber (flax).

Electrospray deposition allowed the proper functionalization of flax fabrics with TiO_2 and CeO_2 NPs, leading to a very homogeneous distribution of these materials, which could be very beneficial in the functionalities of the final system, as the NPs covered all the fabrics' surfaces.





h)

Element	Weight%	Atomic%
C K	49.74	57.22
O K	49.18	42.47
Ti K	1.08	0.31

i)

Element	Weight%	Atomic%
C K	49.25	57.05
O K	48.74	42.41
Ti K	1.03	0.29
CeL	0.98	0.25

Fig. 3. Characterization of the electrospray deposition of the TiO_2 and CeO_2 NPs on flax: a) ATR-FTIR spectra of the flax fabrics (black), flax functionalized with TiO_2 NPs (red) and flax functionalized with TiO_2 and CeO_2 NPs (blue); SEM images of the flax fabrics functionalized with b), d), f) TiO_2 and c), e), g) TiO_2 and CeO_2 NPs (scale bars 100, 50, 10 μm); EDX analysis of the flax fabrics functionalized with h) TiO_2 NPs and with i) TiO_2 and CeO_2 NPs.

3.3. Flax fabrics coated with CS/PEO nanofibers doped with TiO_2 and CeO_2 NPs

Besides the electrospraying method, the production of nanofibers by electrospinning and its deposition onto the fabrics surface was also performed. For this purpose, the polymeric solutions doped with the NPs were optimized and electrospun onto the flax fabrics surface using the parameters: concentration of 0.5 % (w/v) TiO_2 and TiO_2 and CeO_2 NPs, applied voltage of 29 kV, feed rate of 4 mL/h, needle-collector distance of 170 mm and deposition time of 2 h. The characterization of the flax fabrics coated with CS/PEO nanofibers and with the nanofibers doped with TiO_2 and CeO_2 NPs is presented in Fig. 4.

The ATR-FTIR spectra of the flax fabrics coated with the CS/PEO nanofibers and of flax fabrics coated with these nanofibers doped with the TiO_2 and CeO_2 NPs are presented in Fig. 4a. The spectrum of the fabrics only coated with the CS/PEO exhibits not only the peaks of natural cellulosic fibers, namely cellulose, hemicellulose and lignin, but also the characteristic peaks of CS and PEO. The typical bands of the flax fabrics were once again found in the spectrum, as addressed in the analysis of Fig. 3a. Regarding the characteristic bands of CS, the band peaking at around 3300 cm^{-1}, besides being characteristic of natural fibers, can also be attributed to the O—H and N—H stretching vibrations of the CS. On the other hand, the band at around 1550 cm^{-1} is related to the N—H bending of amide II, and the band peaking at 845 cm^{-1} is related to the polymer saccharide region [14,40–47]. The bands related to PEO are the triplet peaks at 1145, 1100, and 1062 cm^{-1} from C-O-C stretching vibrations [14,43,44]. The spectrum of the flax fabrics coated with the CS/PEO nanofibers and doped with the TiO_2 NPs when compared to the previously analysed spectrum shows a new band, peaking at around 450 cm^{-1}, which is characteristic of TiO_2 NPs, as corroborated by the spectrum of Fig. 2. Lastly, and comparing the spectrum of the samples functionalized with only the TiO_2 NPs with the ones functionalized with both NPs, it can be seen the appearance of a band at 550 cm^{-1} characteristic of the Ce—O stretching vibration, which proves the successful functionalization of the CS/PEO coated fabrics with the two types of NPs in the study [38,39]. Once again, there is an increase in the intensity of the band at around 3300 cm^{-1}, likely related to the stretching vibrations of the O—H bonds, proving that hydrogen bonds between the hydroxyl groups of the flax and the CeO_2 NPs were formed [34]. Thus, for the fabrics functionalized with CeO_2, the NPs are more attached to the fibers' surface.

From the GSDR spectra of the flax fabrics coated with the undoped and doped CS/PEO nanofibers (Fig. 4b) it's possible to observe that for the samples with the NPs, a new band appears at approximately 300 nm. This absorption band is characteristic of TiO_2 and CeO_2 NPs, which proves the successful functionalization of flax fabrics coated with CS/PEO electrospun nanofibers with the previously synthesized NPs [45]–[48]. It's also possible to observe that the absorption band decreases for the samples functionalized with the two NPs (TiO_2 and CeO_2) when compared with the samples functionalized with only the TiO_2 NPs. This is probably due to the presence of more NPs and as these materials are inorganic white pigments at nanoscale, they present a higher reflective index. Therefore, with higher quantities of NPs, an increase in reflectance and a consequently decrease in the absorption intensity is expected [49].

The FESEM images of flax fabrics coated with CS/PEO electrospun nanofibers and CS/PEO functionalized with TiO_2 NPs and with TiO_2 and CeO_2 NPs are present in Fig. 4c-g, respectively. It's possible to observe that the formation of the electrospun nanofibers was accomplished and that they were deposited directly onto the flax fabrics surface. The diameter of the nanofibers was measured by the analysis of the FESEM images, using the *Image J* software. It was demonstrated that they presented a mean diameter of 91.3 ± 29.8 nm. In the FESEM image of Fig. 4f-g the presence of the TiO_2 and CeO_2 NPs is clear, with the appearance of sphere-like structures for the functionalized samples, once again proving the successful incorporation of the synthesized NPs. For the samples coated with the two different NPs, it's possible to see that in the fiber's surface, more particles are present, when compared with samples functionalized with only the TiO_2 NPs. This is expected as a higher quantity of NPs was used.

Fig. 4h-j presents the EDX results for the flax fabrics coated with CS/PEO and CS/PEO doped with TiO_2 NPs, respectively. This analysis allowed us to infer the elemental composition of the samples. From the results for the fabrics only coated with the nanofibers, it is possible to observe the presence of C and O, as expected. However, for the samples doped with the NPs it is possible to see the appearance of Ti and Ce characteristics peaks, proof that the functionalization of the flax fabrics coated with CS/PEO nanofibers was successfully achieved.

The ATR-FTIR, GSDR, FESEM, and EDX results confirmed not only the successful formation of electrospun fibers at nanoscale, that were deposited onto the surface of flax fabrics, but also the functionalization of these nanofibers with the NPs. As referred before, electrospinning can improve the anchorage of the NPs on the fabrics surface, and therefore improve the properties of textiles. If the NPs are well attached to the surface of the fabric the functionalities introduced by them will be more long-lasting, which is very beneficial in textile functionalization.

3.4. Functional properties evaluation

3.4.1. Antibacterial activity

The antibacterial activity of metal oxide NPs, like TiO_2 and CeO_2 has already been reported since these nanomaterials present photocatalytic activity [50–54]. The reactive oxygen species (ROS) generated during this process can attack organic compounds present in bacteria, specifically cell membranes, RNA, DNA, proteins, and lipids, which consequently results in cell death. Gram-negative and gram-positive bacteria present a negatively charged cell wall, which influences the interactions between them and the positive ions released by the NPs. In the specific case of Gram-negative bacteria, there is the presence of a mosaic of anionic surfaces on the cell wall, instead of a continuous layer. Thus, higher amounts of NPs can bind to these sites, increasing the local toxicity [1,55,56]. As such, the antibacterial activity of the flax fabrics functionalized with TiO_2 and CeO_2 NPs by the electrospraying deposition method was assessed, and the results are shown in Table 3.

From the results of Table 3, it's possible to verify that all the samples presented bacteriostatic activity against both bacteria. However, with the introduction of the NPs there is an enhancement of the antibacterial activity of flax fabrics. These materials by themselves present some antimicrobial properties, as already reported [23,57,58], being that this is most likely related to the phenolic content of the lignin present in blast fibers. Nonetheless, the functionalization with TiO_2 and CeO_2 was essential for the improvement of the antibacterial activity, especially in the case of Gram-positive bacteria. Besides, it is not possible to conclude about the individual effect of each type of NPs because there is no significant difference between the values of using only TiO_2 and the combination effect of TiO_2/CeO_2.

Regarding the coating of flax fabrics with the nanofibers produced by electrospinning process, CS was used as the main polymer for the formulation's development. In fact, CS has emerged as one of the most interesting materials due to its excellent characteristics, especially its antimicrobial activity. This property has already been described in literature and the main antimicrobial mechanisms proposed are the chelating properties of CS and the interaction between the CS and microbial DNA. This affects the synthesis of mRNA, and therefore the synthesis of proteins and the electrostatic interaction between the negatively charged microbial cell membranes, leading to the leaking of intracellular elements and finally to cell death. Several reports of the antibacterial activity of CS have already been demonstrated in the literature [14,40,41]. Table 4 shows the antibacterial results of flax fabrics functionalized with CS/PEO nanofibers.

Table 4 shows that all the samples presented bactericidal activity not only against the Gram-positive bacteria *Staphylococcus aureus*, but also

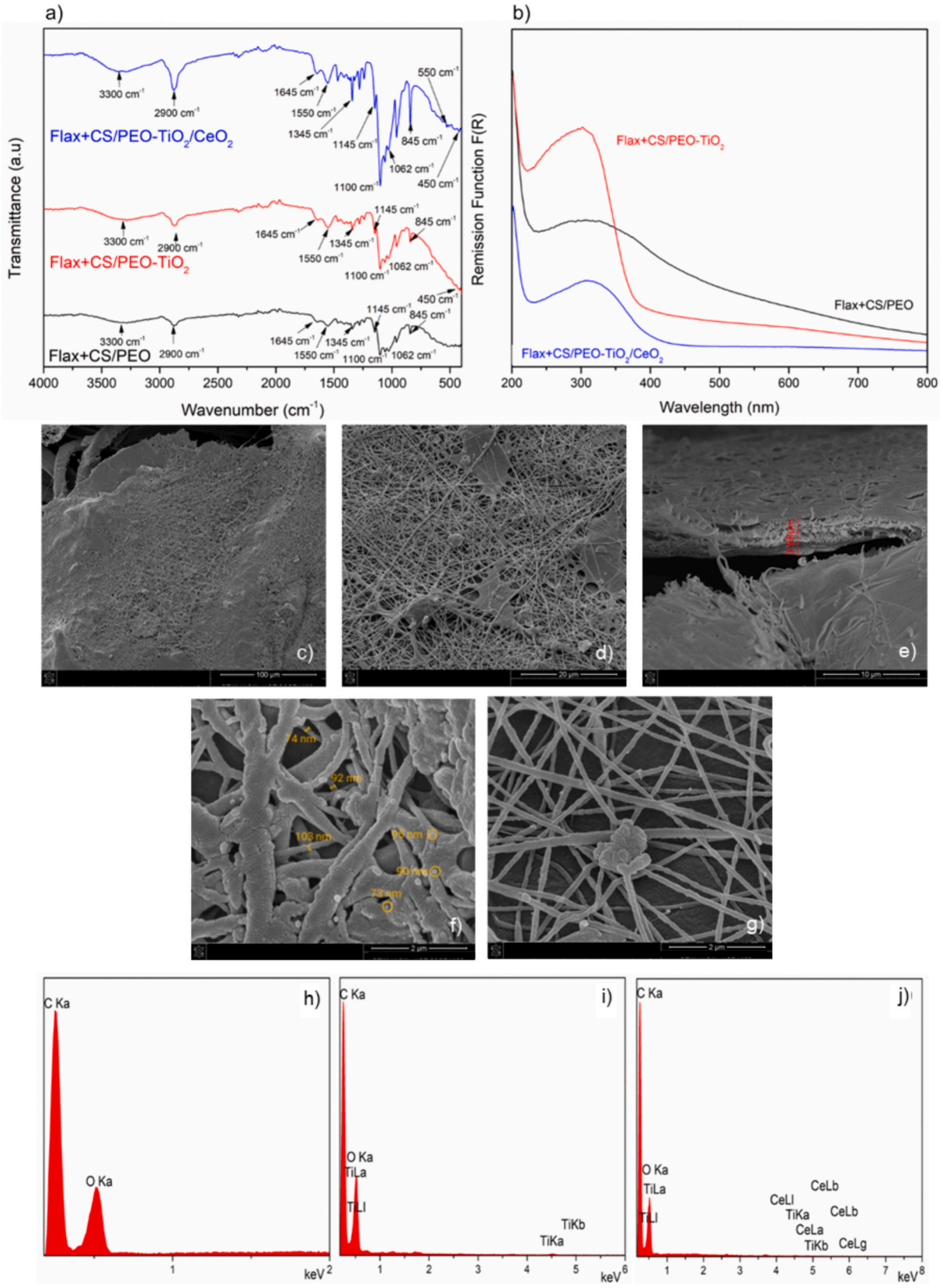


Fig. 4. Characterization of the flax fabrics coated with CS/PEO nanofibers doped with TiO_2 and CeO_2 NPs: a) ATR-FTIR spectra of the flax fabrics coated with CS/PEO nanofibers (black), flax coated with CS/PEO doped with TiO_2 NPs (red) and flax coated with CS/PEO doped with TiO_2 and CeO_2 NPs (blue); b) GSDR spectra of the flax fibers coated with CS/PEO nanofibers (black), flax coated with CS/PEO doped with TiO_2 NPs (red) and flax coated with CS/PEO doped with TiO_2 and CeO_2 NPs (blue); c), d), e) FESEM images of the flax fibers coated with CS/PEO nanofibers (scale bars 100, 20, and 10 μm); FESEM images of the flax fabrics coated with CS/PEO nanofibers functionalized with f) TiO_2 NPs and with g) TiO_2 and CeO_2 NPs (scale bar 2 μm); EDX analysis of flax fabrics with h) CS/PEO, with i) CS/PEO and TiO_2 NPs and j) CS/PEO and TiO_2 and CeO_2 NPs.

Table 3
Antibacterial activity (%) values of flax, flax+TiO_2 and flax+TiO_2-CeO_2 samples (electrospraying method) against *Staphylococcus aureus* and *Escherichia coli*. Significant differences in antibacterial activity between the different samples were detected by two-way ANOVA followed by Tukey's post-hoc test (sample * bacteria interaction), with $p < 0.001$ for Flax+TiO_2 NPs and Flax+TiO_2-CeO_2 against Flax alone.

Sample	*Staphylococcus aureus*	*Escherichia coli*
Flax	84.73 ± 6.31	93.66 ± 5.5
Flax+TiO_2	99.86 ± 0.09	99.25 ± 0.49
Flax+TiO_2-CeO_2	98.94 ± 0.70	99.24 ± 0.81

Table 4
Antibacterial activity (%) values of flax+CS/PEO, flax+CS/PEO-TiO_2 and flax+CS/PEO-TiO_2/CeO_2 samples (electrospinning method) against *Staphylococcus aureus* and *Escherichia coli*. No significant differences in antibacterial activity were detected between the different samples (two-way ANOVA followed by Tukey's post-hoc test, sample * bacteria interactions).

Sample	*Staphylococcus aureus*	*Escherichia coli*
Flax+CS/PEO	99.97 ± 0.0	100.0 ± 0.0
Flax+CS/PEO-TiO_2	99.96 ± 0.01	100.0 ± 0.0
Flax+CS/PEO-TiO_2/CeO_2	99.97 ± 0.02	100.0 ± 0.0

against the Gram-negative bacteria *Escherichia coli*. In fact, comparing the flax fabrics with or without NPs, there is no evidence of NPs influence. There was no significant difference between the flax fabrics functionalized with only the CS/PEO nanofibers and the ones functionalized with the nanofibers doped with the TiO_2 and CeO_2 NPs. This is probably related to the excellent intrinsic antibacterial properties of CS, which are already enough to develop an antibacterial material. However, for higher bacterial loads, or after use/time/wash, having three anti-bacterial compounds would still prove to be beneficial. Moreover, the introduction of the NPs didn't affect this property, allowing the production of a natural fiber-based fabric with excellent antibacterial properties. By the comparison of these results with the results obtained for the flax fabrics functionalized by electrospraying (Table 3) is possible to conclude that the coating with CS nanofibers was more beneficial in the antibacterial activity of the developed samples.

3.4.2. Methylene blue degradation

Besides the activity against biological agents, the potential of these fabrics to be used as decontaminants of chemical agents was also accessed. Firstly, MB was used as the model compound for photocatalytic evaluation, since it presents an obvious colour change. To do that, 500 μL of a MB solution was dropped onto each fabric sample and kept in the dark for 30 min. to ensure the adsorption-desorption equilibrium. Afterwards, the samples were kept under UV radiation for 24 h and monitored by GSDR. This monitorization was made hourly until the 7 h' time, and the last measurement was made after 24 h. The results of the flax fabrics functionalized with TiO_2 and CeO_2 NPs by electrospray deposition are represented in Fig. 5 b-d. For the flax functionalized with CS/PEO nanofibers doped with TiO_2 and CeO_2 NPs the results are represented in Fig. 6 b-d. The absorbance spectrum of the MB solution used was also measured, as the control (Fig. 5 and Fig. 6a).

The spectrum of the MB solution shows the characteristic absorption peaks of this dye, at around 615 and 664 nm, as expected [34,59,60]. When comparing the spectrum of the non-functionalized flax (Fig. 5b) with the spectra of the functionalized ones (Fig. 5c-d), it's possible to verify that there is a faster decrease in the intensity of the MB peaks for the samples with NPs.

Comparing the spectrum of flax/CS/PEO nanofibers with the spectra of fabrics with NPs, (Fig. 6 b-d) it's possible to infer that the intensity of the characteristic MB bands peaking at 615 and 664 nm decreases faster for the samples with NPs. In fact, after 2 h of irradiation, the remission function value for the maximum peaking at 664 nm was 12.10 for the flax+CS/PEO, 6.07 for the flax+CS/PEO-TiO_2 and of 2.40 for the flax+CS/PEO-TiO_2/CeO_2. There was an intense decrease in the absorption intensity of these bands indicating the strongest degradation behavior of the fabrics when the NPs are present at their surface. This is most likely related to the photocatalytic activity of the TiO_2 and CeO_2 NPs, which leads to the degradation of the MB, instead of only its absorption. Additionally, it's possible to observe that this reduction of intensity is even faster and more accentuated for the sample doped with the two types of NPs, which is probably related to the synergistic effect, with the CeO_2 NPs improving the properties of the TiO_2 NPs [5]. It's important to notice that the results of the samples coated with the nanofibers are better than the ones functionalized by electrospray deposition, which is probably related to the higher surface area of the electrospun fibers, as well as better filtration properties. Since the deposited fibers were nanometric, smaller particles can be captured in the pores of the electrospun membrane, since the fibers/pores are also smaller. A very high surface area to volume ratio results in a higher surface cohesion, which also allows more particles to be trapped in the fibrous structure [61].

The photodegradation of MB by TiO_2 NPs [62–65] and CeO_2 [66–68] has already been reported. TiO_2 is one of the most used materials for photocatalysis since, besides presenting low toxicity and cost, it is chemically stable. In addition, it has an optical band gap energy (E_g) that is suitable for effective photodegradation. Besides the wide band gap of TiO_2 (3.2 eV), these NPs are only able to absorb UV radiation, which corresponds to a small percentage of sunlight (3–5 %). Moreover, they present a high rate of pair hole-electron recombination, not favorable for photocatalysis [5,69].

On the other hand, CeO_2 absorbs mainly in the visible range, being that the combination of TiO_2 with this material can improve the light absorption range. This combination can also promote charge separation and narrow the band gap by semiconductor heterojunction, leading to a more efficient photocatalysis process [5]. Thus, the addition of CeO_2 to TiO_2 could be very beneficial for its photocatalytic behavior.

The possible photocatalytic process of the flax samples functionalized with CS/PEO nanofibers doped with TiO_2 and CeO_2 NPs can be explained by the *Z*-scheme heterojunction, as shown in Fig. 7. In contrast to the traditional type II heterojunction scheme, the Z-scheme mechanism is currently more used to describe the photocatalytic process. This is due to its worth in explaining the effective charge separation of photogenerated charge carriers. It is expected that the photoexcited electron in TiO_2's conduction band and the photogenerated hole in CeO_2's valence band recombine. Resulting in the generation of the highly reactive species $O_2^{\cdot}$ by the photoexcited electrons accumulated on the conduction band in CeO_2. Due to the charge accumulation on the TiO_2 valence band, the photocatalytic process produces the reactive species $OH^{\bullet}$ concurrently. As a result, the MB dye is degraded by the reactive species that were produced [5,70,71].

3.4.3. DMMP degradation

DMMP is usually used as a simulant for nerve agents since it presents a similar chemical structure but a lower toxicity. Therefore, to avoid harmful effects during research, the degradation of DMMP is the best way to test the possible degradation of nerve agents, namely sarin gas. In this work, the samples that obtained the best photocatalytic activity and antibacterial activity results, flax coated with CS/PEO nanofibers doped with TiO_2 and CeO_2 NPs were tested for the degradation of DMMP. The quantification of the simulant agent was made by GC–MS after 0, 1, 2, 3, 4, 5, 6, 18 and 24 h under UV radiation. The same was made without any fabric as the control (Fig. 8).

From the results of Fig. 8 it's possible to verify that when comparing the results of the flax fabrics coated with the doped nanofibers with the results of the control, there is a higher decrease in the DMMP quantity over time. For the control, the DMMP quantity remained almost the same even after the 24 h period (1090 μg). However, for the flax fabrics

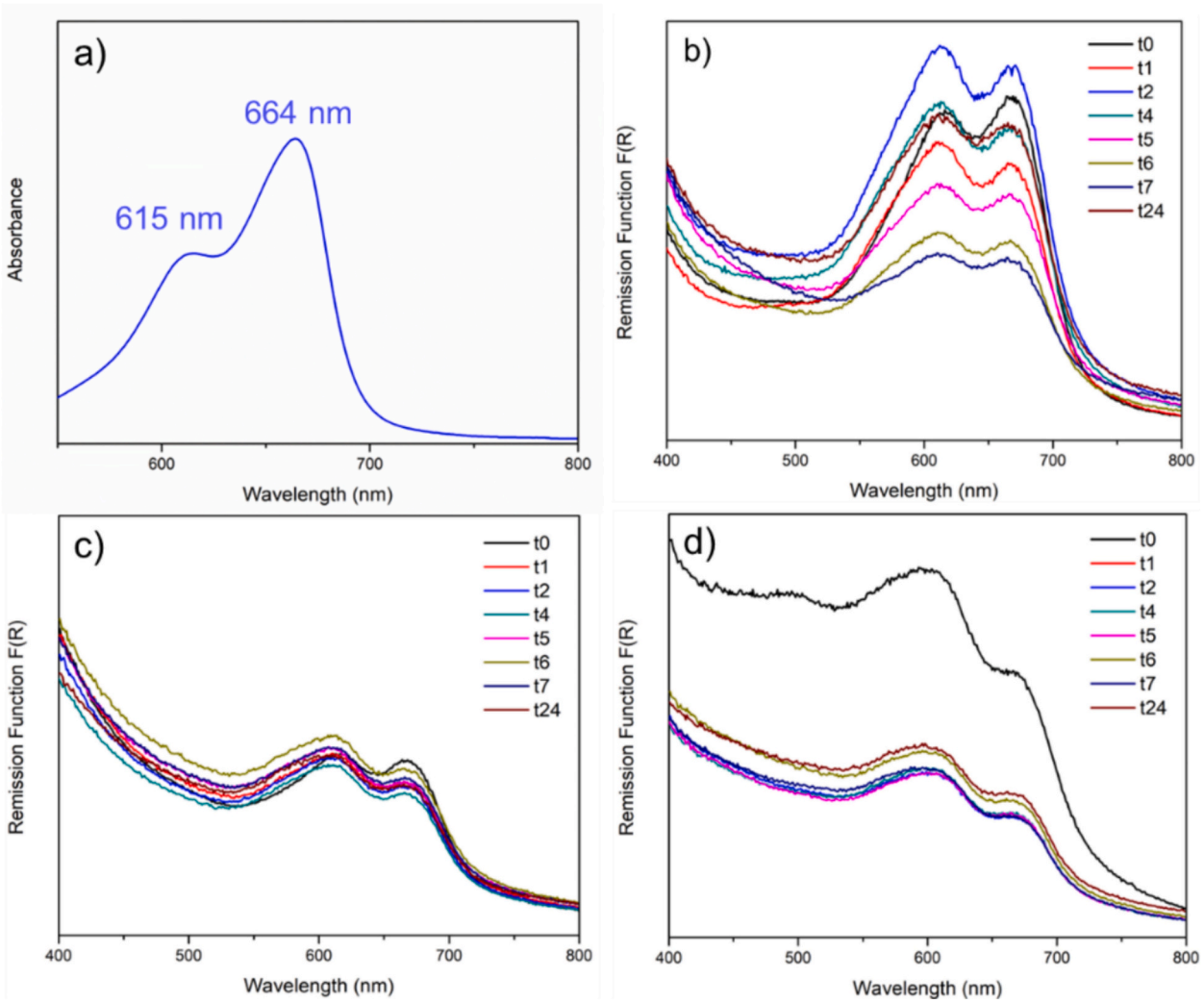


Fig. 5. a) Absorbance spectrum of the MB solution (control); GSDR spectra of the b) non-functionalized flax fabrics c) flax functionalized with TiO_2 NPs and d) flax functionalized with TiO_2 and CeO_2 NPs by electrospray deposition in contact with MB after 0, 1, 2, 4, 5, 6, 7 and 24 h. Significant differences in degradation capacity between the different samples were detected by two-way ANOVA followed by Tukey's post-hoc test (sample * time-point interaction, with $p < 0.001$ for all comparisons).

functionalized with the CS/PEO-TiO_2/CeO_2 nanofibers the DMMP quantity decreased over time, being only 24.2 μg after 24 h of UV radiation. During this time period, the flax fabric coated with CS/PEO-TiO_2/CeO_2 nanofibers was able to degrade 97.82 % of DMMP. As far as it is known, there is no evidence in the literature regarding the use of functionalized natural fabrics for this purpose and we strongly believe that these materials are of great importance for the development of active personal protective equipment against chemical and biological hazardous agents.

The DMMP's adsorption and degradation on metal oxide NPs have already been reported in the literature using isolated nanomaterials [72–76]. These materials have improved absorptive and reactive properties towards toxic compounds due to their high surface area, numerous reactive edges, corner defects, and acid and base sites and hydroxyl groups on their surface. Chemical and biological hazardous agents that get trapped in sorbent pores undergo reactions that are aided by reactive sites integrated with metal oxide NPs, neutralizing their toxic characteristics and bactericidal effect [77]. The interaction of DMMP with metal oxides has been the subject of several experimental investigations, but little is known about the mechanisms leading to the decomposition of DMMP and the impact of surface shape and electrical characteristics on these processes. It is generally acknowledged that DMMP initially interacts with an oxide surface through its phosphoryl oxygen and forms a bond with one of the Lewis acid sites on the surface (for example, an under-coordinated metal atom). On the other hand, the main decomposition mechanism of DMMP is typically attributed to the breaking of a P-OCH_3 bond through an electrophilic or nucleophilic attack involving surface hydroxyls. At normal temperatures, DMMP breakdown on oxide surfaces mostly produces methanol, dimethyl ether, and surface methoxy groups (Fig. 9) [78,79]. It is important to highlight that these tests were only preliminary and further research is needed to draw more in-depth conclusions regarding the degradation of DMMP by the developed samples. Nonetheless, these results seem to be very promising for the development of personal protective equipment, since they can degrade chemical hazardous agents, which is essential for the obtention of active protection, instead of a passive one. Moreover, taking into consideration that in this work NPs and nanofibers were used, protective fabrics are obtained without adding extra weight, which is of great importance in the development of personal protection equipment [1].

3.4.4. Wash fastness

The durability of the functionalization of the flax with nanofibers doped with TiO_2 and TiO_2/CeO_2 NPs was evaluated since these were the samples that presented the best results of antibacterial activity and MB degradation. To do so, the samples were immersed in distilled water and were centrifugated in order to mimic domestic washing (as described in

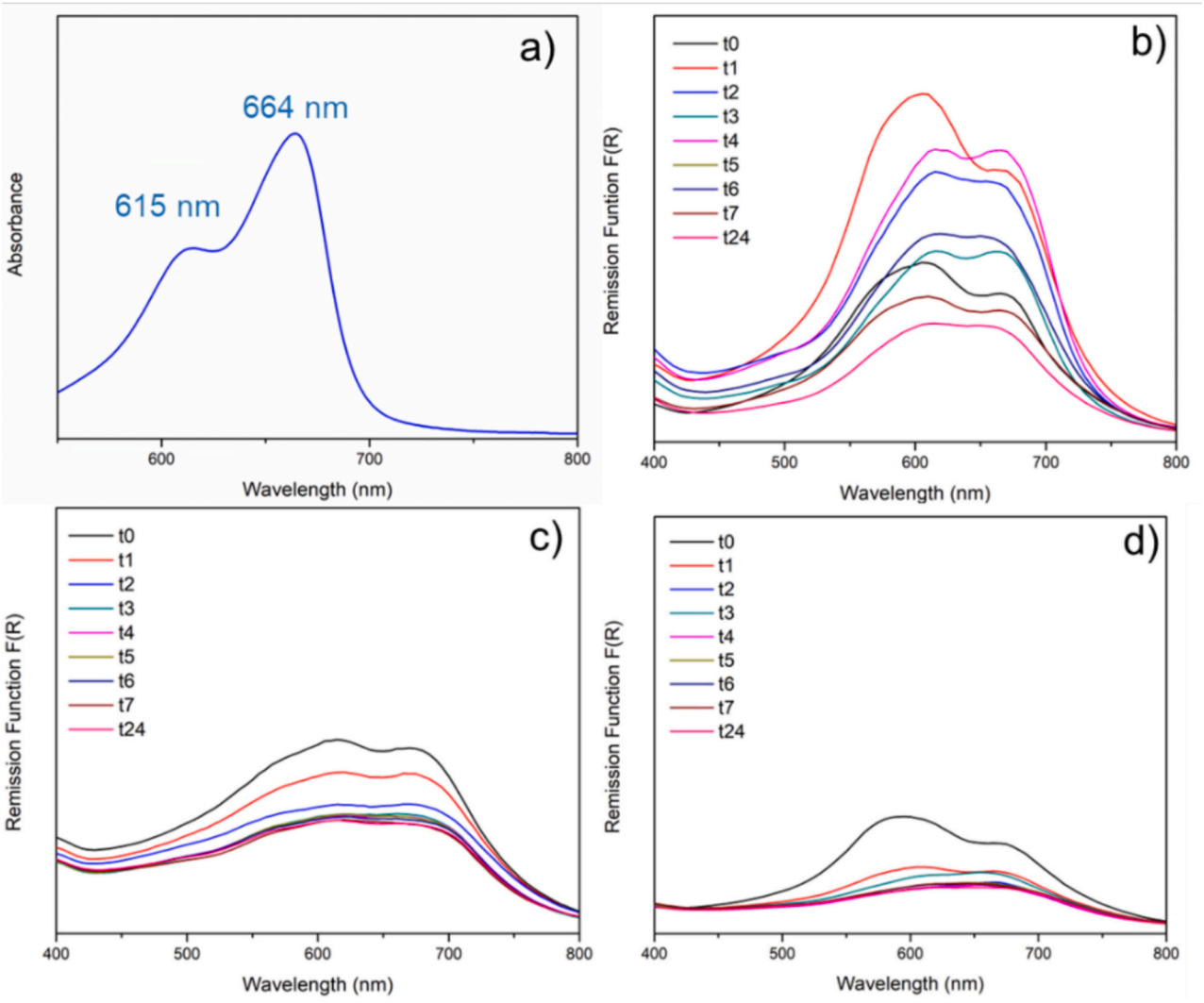


Fig. 6. a) Absorbance spectrum of the MB solution (control); GSDR spectra of the b) flax functionalized with CS/PEO nanofibers, c) flax functionalized with CS/PEO nanofibers doped with TiO_2 NPs and d) flax functionalized with CS/PEO nanofibers doped with TiO_2 and CeO_2 NPs in contact with MB after 0, 1, 2, 3, 4, 5, 6, 7 and 24 h. Significant differences in degradation capacity between the different samples were detected by two-way ANOVA followed by Tukey's post-hoc test (sample * time-point interaction, with $p < 0.001$ for all comparisons).

2.9). Several aliquots of the washing solution were taken, and their absorbance was measured, in order the calculate the NPs' loss percentage. The obtained spectra, after 1, 2, 4, 5, 6, 7, and 24 h of the washing cycle are represented in Fig. 10a-b.

Analysing the two spectra it's possible to verify that the intensity of the peak at around 280 nm (characteristic of the studied NPs) increases over time. This indicates that more particles are being gradually released in the washing solution, as was expected. Nevertheless, even after 24 h in direct contact with distilled water, there were still NPs present on the fabrics' surface. This washing process is essential to remove the NPs that are loose on the surface of the fabrics, leaving only those that stay strongly attached to the surface. However, looking at the spectrum of the flax+CS/PEO-TiO_2/CeO_2 (Fig. 10b) it can be observed that the intensity of the NPs' characteristic peak stays the same after the 5 h' time. For the spectrum of the flax+CS/PEO-TiO_2 (Fig. 10a) this only happens at 7 h' time. Therefore, the release of the NPs in the washing solution lasts longer for the samples functionalized with only TiO_2, being that the introduction of the CeO_2 the anchorage of the NPs onto the fabrics surface increases. This is also corroborated by the values of the NPs' loss percentages, which were 32.5 % for the samples with TiO_2 and 27.4 % for the samples with TiO_2 and CeO_2 NPs and by the ATR-FTIR results. Therefore, the addition of the CeO_2 NPs in the developed samples was very beneficial, leading to better NPs adhesion, without compromising their excellent properties.

4. Conclusions

The main aim of this work was the development of a fibrous structure able to degrade chemical and biological agents based on natural fibers and metal oxide NPs. In this sense, flax fabrics were functionalized with TiO_2 and CeO_2 NPs by electrospray deposition, and CS/PEO nanofibers were doped with the same NPs. As far as the authors know, this is currently not reported in the literature. The TiO_2 NPs were synthesized by a very straightforward precipitation method and were electrosprayed and incorporated in the biopolymeric formulation, which was then electrospun onto the flax fibers surface. CeO_2 NPs were also added to improve the characteristics of the TiO_2.

The TiO_2 NPs were successfully synthesized and presented a spherical morphology. It was possible to not only verify the successful functionalization of the fabrics with TiO_2 and CeO_2 by electrospray deposition but also to conclude that CS/PEO nanofibers were indeed formed onto the surface of the flax and that the two NPs were incorporated in these electrospun nanofibers. The washing durability of the nanocoating that was applied on the flax fabrics was also evaluated, and

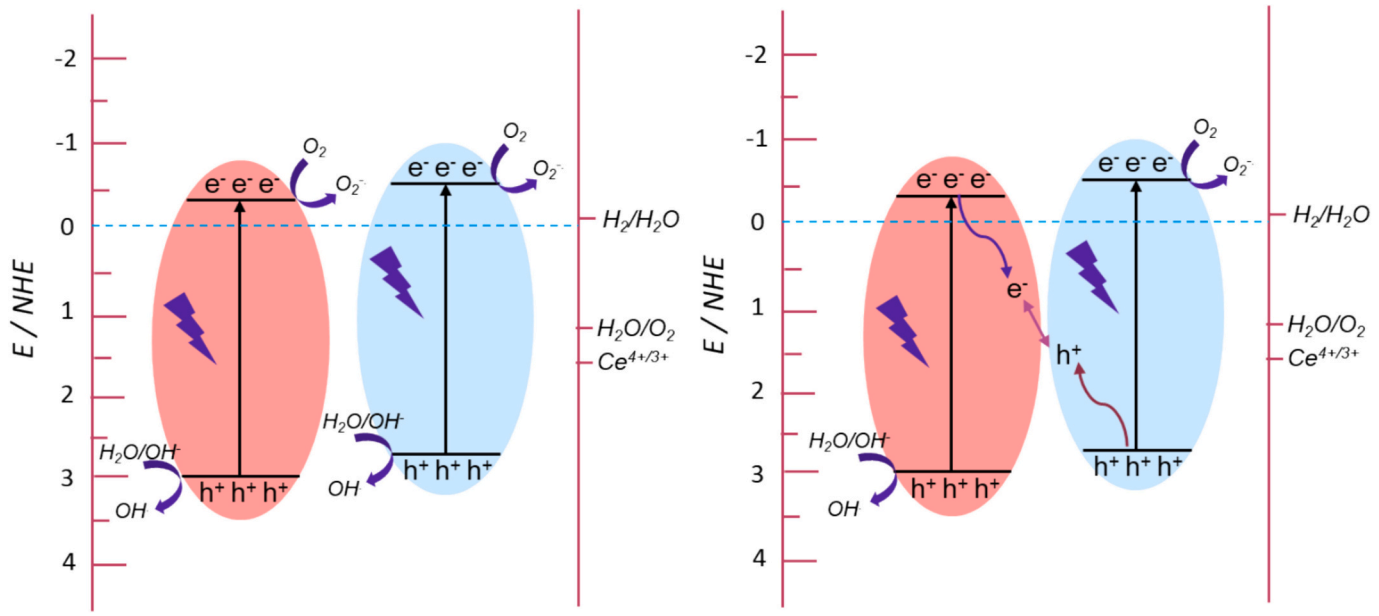


Fig. 7. Schematic diagram of the photocatalytic mechanism of a) heterojunction-type II b) and direct Z-scheme of the TiO_2-CeO_2 nanocomposite.

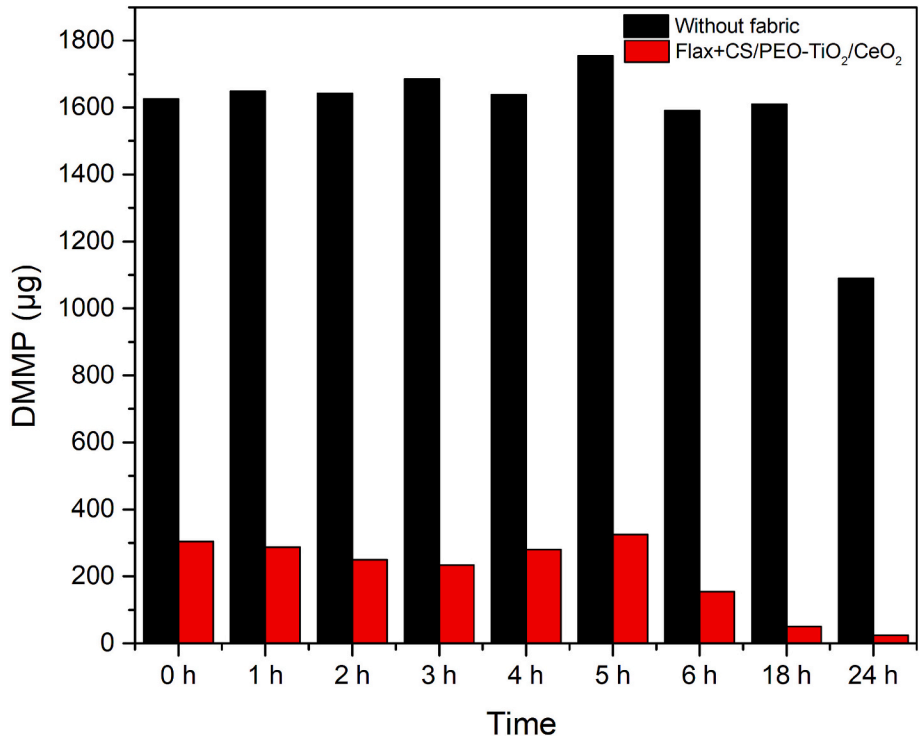


Fig. 8. DMMP quantification (µg) after 0, 1, 2, 3, 4, 5, 6, 18 and 24 h of UV radiation without the presence of any sample (black) and for the flax fabrics coated with CS/PEO nanofibers doped with TiO_2 and CeO_2 NPs (red). Significant differences in degradation capacity between the different samples were detected by two-way ANOVA followed by Tukey's post-hoc test (sample * time-point interaction, with $p < 0.001$ for all comparisons).

it was verified that the addition of the CeO_2 improved the anchorage of the NPs onto the fibers' surface.

The developed samples presented antibacterial activity. The degradation of hazardous chemical agents was also tested, using MB as a model compound and DMMP. The samples that presented the best performance in the protection against chemical and biological agents were the ones coated with nanofibers and with TiO_2 and CeO_2 NPs.

Essentially, this work presents the development of natural fibers functionalized with metal oxide NPs and with bio-based polymeric nanofibers doped with the same nanomaterials. The TiO_2 NPs were synthesized using a very simple method and using mild conditions, namely water as solvent and low reaction times and calcination temperatures. Besides the homogenous distribution ensured by the electrospray deposition, the electrospinning nanofibers allowed a higher surface area, as well as antibacterial activity, due to the CS characteristics. The addition of the CeO_2 was also of great importance to improve not only the anchorage of the NPs, but also the photodegradation efficiency of the TiO_2 NPs. Therefore, the developed materials present great

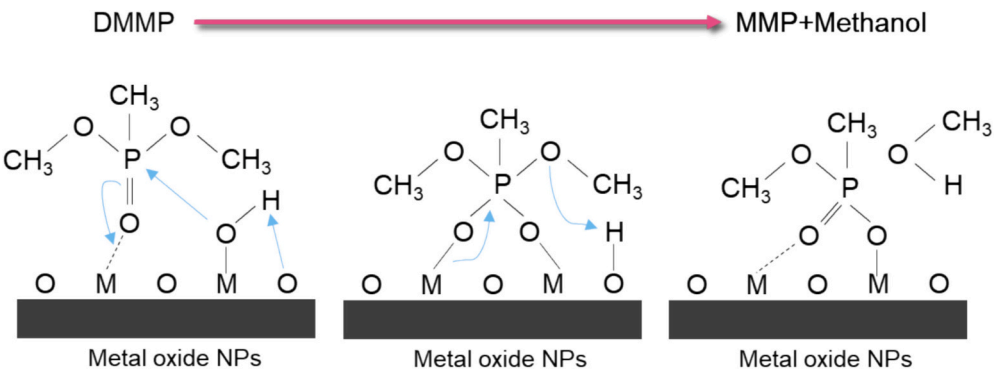


Fig. 9. Schematic diagram showing of the decomposition of DMMP on the surface of metal oxide NPs [78].

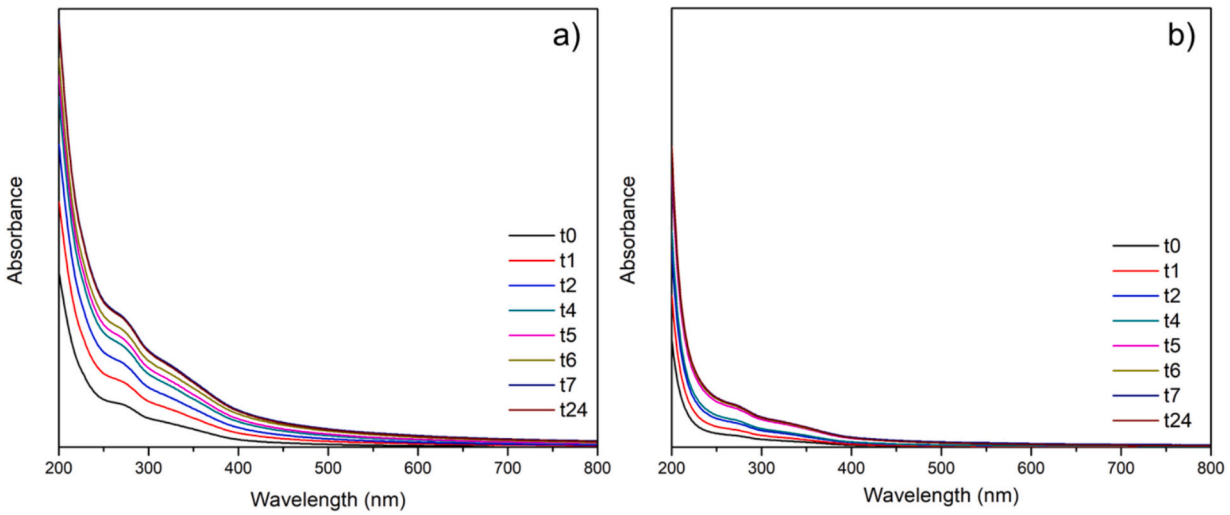


Fig. 10. Absorbance spectra of washing water of the flax fabrics coated with CS/PEO nanofibers doped with a) TiO_2 NPs and b) TiO_2/CeO_2 NPs after 1, 2, 4, 5, 6, 7, 24 h in contact with distilled water and centrifugated at 200 rpm.

potential to be used in the development of active personal protective equipment.

Funding

The authors are thankful to project UID/CTM/00264/2023 of 2C2T – Centro de Ciência e Tecnologia Têxtil, funded by National Founds through FCT/MCTES and to the FCT PhD Scholarship (grant number SFRH/BD/147812/2019) of Joana Araújo (https://doi.org/10.54499/SFRH/BD/147812/2019). Diana Ferreira is thankful to CEECIND/02803/2017 (https://doi.org/10.54499/CEECIND/02803/2017/CP1458/CT0003). Pilar Teixeira is also thankful to FCT, under the scope of the strategic funding of UIDB/04469/2020 unit. Cátia A.L. Graça thanks FCT funding under the Scientific Employment Stimulus – Individual Call 2022.08029.CEECIND (https://doi.org/10.54499/2022.08029.CEECIND/CP1733/CT0010). The authors are also thankful to LA/P/0045/2020 (ALiCE), UIDB/50020/2020 and UIDP/50020/2020 (LSRE-LCM), funded by national funds through FCT/MCTES (PIDDAC) and to the Advanced Electron Microscopy, Imaging, and Spectroscopy (AEMIS) from INL for their support. Finally, the authors thank the project GIATEX (Gestão Inteligente da Água na ITV, C644943052-00000050) and Project DRI/India/0447/2020 (https://doi.org/10.54499/DRI/India/0447/2020).

The authors have no relevant financial or non-financial interests to disclose.

CRediT authorship contribution statement

Joana C. Araújo: Writing – original draft, Methodology, Investigation, Conceptualization. **Pedro M. Silva:** Writing – review & editing, Methodology. **Miguel A. Cerqueira:** Writing – review & editing, Methodology. **Pilar Teixeira:** Writing – review & editing, Methodology. **Vânia Tira-Picos:** Methodology. **Pedro Neto:** Methodology. **Olívia Salomé G.P. Soares:** Writing – review & editing, Methodology. **Cátia L. Graça:** Writing – review & editing, Methodology. **Raul Fangueiro:** Supervision, Funding acquisition. **Diana P. Ferreira:** Writing – review & editing, Supervision, Funding acquisition.

Declaration of competing interest

The authors declare the following financial interests/personal relationships which may be considered as potential competing interests: Diana P. Ferreira reports financial support was provided by Foundation for Science and Technology. Joana C. Araujo reports financial support was provided by Foundation for Science and Technology. Pilar Teixeira reports financial support was provided by Foundation for Science and Technology. Catia L. Graca reports financial support was provided by Foundation for Science and Technology. Olivia Salome G. P. Soares reports was provided by Foundation for Science and Technology. If there are other authors, they declare that they have no known competing financial interests or personal relationships that could have appeared to influence the work reported in this paper.

Data availability

The raw/processed data required to reproduce these findings cannot be shared at this time as the data also forms part of an ongoing study.

References

[1] J.C. Araújo, R. Fangueiro, D.P. Ferreira, Protective multifunctional fibrous systems based on natural fibers and metal oxide nanoparticles, Polymers 13 (16) (2021), https://doi.org/10.3390/polym13162654.

[2] Y. Nam, H. Lim, C. Ko, J.Y. Lee, Photocatalytic activity of TiO2 nanoparticles: a theoretical aspect, J. Mater. Chem. A 7 (2019) 13833–13859, https://doi.org/10.1039/c9ta03385h.

[3] S. Pansambal, et al., Bioengineered cerium oxide (CeO2) nanoparticles and their diverse applications: a review, Appl. Nanosci. (2022), https://doi.org/10.1007/s13204-022-02574-8.

[4] A. Dhall, W. Self, Cerium oxide nanoparticles: a brief review of their synthesis methods and biomedical applications, Antioxidants (Basel, Switzerland) 7 (8) (2018), https://doi.org/10.3390/antiox7080097.

[5] B. Aljawrneh, A. Alsaad, B. Albiss, S. Alrousan, A. Alshanableh, S. Mutlaq, Cellulose acetate membranes treated with titanium dioxide and cerium dioxide nanoparticles and their nanocomposites for enhanced photocatalytic degradation activity of methylene blue, J. Mater. Sci. Mater. Electron. 33 (14) (2022) 11420–11433, https://doi.org/10.1007/s10854-022-08115-x.

[6] N. Thakur, et al., A critical review on the recent trends of photocatalytic, antibacterial, antioxidant and nanohybrid applications of anatase and rutile TiO2 nanoparticles, Sci. Total Environ. 914 (2024) 169815, https://doi.org/10.1016/j.scitotenv.2023.169815.

[7] M. Kumar, S. Loganathan, D. Prakash, D. Natarajan, Antibacterial and anticancer potential of mycosynthesized titanium dioxide (TiO2) nanoparticles using Hypsizygus ulmarius, Biomass Convers. Biorefinery 14 (12) (2022), https://doi.org/10.1007/s13399-022-03186-6.

[8] D.F. Baamer, E.T. Helmy, M.M.M. Mostafa, J.H. Pan, Synthesis of TiO2 nanoparticles using different routes with enhanced photocatalytic and antibacterial properties, Ceram. Int. 50, no. 9, Part B (2024) 15780–15789, https://doi.org/10.1016/j.ceramint.2024.02.058.

[9] N. Korkmaz, D. Kısa, Y. Ceylan, E. Güçlü, F. Şen, A. Karadağ, Synthesis of CeO2 nanoparticles from hemp leaf extract: evaluation of antibacterial, anticancer and enzymatic activities, Inorg. Chem. Commun. 159 (2024) 111797, https://doi.org/10.1016/j.inoche.2023.111797.

[10] C. Song, S. Luo, M. He, X. Zhao, M. Sun, Antibacterial mechanism of water-soluble CeO2 nanoflowers and its product design in antibacterial application, Appl. Surf. Sci. 679 (2025) 161249, https://doi.org/10.1016/j.apsusc.2024.161249.

[11] S. Zeng, A. Shui, H. Yu, C. He, Sonochemical synthesis of CeO2 nanoparticles with high photocatalytic and antibacterial activities under visible light, Int. J. Appl. Ceram. Technol. 21 (5) (2024) 3141–3151, https://doi.org/10.1111/ijac.14775.

[12] S.M. Costa, R. Fangueiro, D.P. Ferreira, Drug delivery Systems for Photodynamic Therapy: the potentiality and versatility of electrospun nanofibers, Macromol. Biosci. 22 (5) (2022) 2100512.

[13] S.M. Costa, et al., Antibacterial and biodegradable electrospun filtering membranes for facemasks: an attempt to reduce disposable masks use, Appl. Sci. 12 (1) (2022) 67.

[14] A.S. Ribeiro, et al., Chitosan/nanocellulose electrospun fibers with enhanced antibacterial and antifungal activity for wound dressing applications, React. Funct. Polym. 159 (2021) 104808, https://doi.org/10.1016/j.reactfunctpolym.2020.104808.

[15] M.A. Matica, F.L. Aachmann, A. Tøndervik, H. Sletta, V. Ostafe, Chitosan as a wound dressing starting material: antimicrobial properties and mode of action, Int. J. Mol. Sci. 20 (23) (2019), https://doi.org/10.3390/ijms20235889.

[16] N.P. Rijal, U. Adhikari, N. Bhattarai, J.A. Jennings, J.D. Baa, T.-C. Baa, B. V. Bumgardner (Eds.), 9 - Production of Electrospun Chitosan for Biomedical Applications, Woodhead Publishing, 2017, pp. 211–237.

[17] N. Amiri, et al., Teicoplanin-loaded chitosan-PEO nanofibers for local antibiotic delivery and wound healing, Int. J. Biol. Macromol. 162 (2020) 645–656.

[18] M. Pakravan, M.-C. Heuzey, A. Ajji, A fundamental study of chitosan/PEO electrospinning, Polymer (Guildf). 52 (21) (2011) 4813–4824.

[19] S.K. Boda, X. Li, J. Xie, Electrospraying an enabling technology for pharmaceutical and biomedical applications: a review, J. Aerosol Sci. 125 (2018) 164–181, https://doi.org/10.1016/j.jaerosci.2018.04.002.

[20] J.A. Tapia-Hernández, et al., Micro- and nanoparticles by electrospray: advances and applications in foods, J. Agric. Food Chem. 63 (19) (2015) 4699–4707, https://doi.org/10.1021/acs.jafc.5b01403.

[21] S.M. Costa, D.P. Ferreira, A. Ferreira, F. Vaz, R. Fangueiro, Multifunctional flax fibres based on the combined effect of silver and zinc oxide (Ag/ZnO) nanostructures, Nanomaterials (2018) 1–21, https://doi.org/10.3390/nano8121069.

[22] A.P. More, Flax fiber–based polymer composites: a review, Adv. Compos. Hybrid Mater. 5 (1) (2022) 1–20, https://doi.org/10.1007/s42114-021-00246-9.

[23] M.Q. Tusief, N. Amin, M. Abass, Antimicrobial studies of knitted fabrics from bamboo, soybean and flax fibers at various blends, J. Text. Sci. Eng. 5 (3) (2015).

[24] Y. Ci, S. Wang, X. Zhang, Z. Fang, A. Ma, Z. Huang, Chemical warfare agents' degradation on Fe–cu codoped TiO2 nanoparticles, Appl. Phys. A 124 (11) (2018) 786, https://doi.org/10.1007/s00339-018-2209-x.

[25] S. Balu, K. Uma, G.-T. Pan, T.C.-K. Yang, S.K. Ramaraj, Degradation of methylene blue dye in the presence of visible light using SiO2@α-Fe2O3 nanocomposites deposited on SnS2 flowers, Materials 11 (6) (2018), https://doi.org/10.3390/ma11061030.

[26] J. Restivo, C.A. Orge, A.S.G.G. Santos, O.S.G.P. Soares, M.F.R. Pereira, Nano- and macro-structured cerium oxide – carbon nanotubes composites for the catalytic ozonation of organic pollutants in water, Catal. Today 384–386 (2022) 187–196, https://doi.org/10.1016/j.cattod.2021.04.012.

[27] L. Yang, B. Kruse, Revised Kubelka–Munk theory. I. Theory and application, J. Opt. Soc. Am. 21 (10) (2004) 1933–1941.

[28] W. Buraso, V. Lachom, P. Siriya, P. Laokul, Synthesis of TiO2 nanoparticles via a simple precipitation method and photocatalytic performance, Mater. Res. Express 5 (11) (2018) 115003, https://doi.org/10.1088/2053-1591/aadbf0.

[29] T. Raguram, K.S. Rajni, Synthesis and analysing the structural, optical, morphological, photocatalytic and magnetic properties of TiO2 and doped (Ni and cu) TiO2 nanoparticles by sol–gel technique, Appl. Phys. A Mater. Sci. Process. 125 (5) (2019) 288, https://doi.org/10.1007/s00339-019-2581-1.

[30] L. Chougala, M. Yatnatti, R. Linganagoudar, R. Kamble, J. Kadadevarmath, A simple approach on synthesis of TiO2 nanoparticles and its application in dye sensitized solar cells, J. Nano- Electron. Phys. 9 (2017) 4001–4005, https://doi.org/10.21272/jnep.9(4).04005.

[31] A. León, et al., FTIR and Raman characterization of TiO2 nanoparticles coated with polyethylene glycol as carrier for 2-Methoxyestradiol, Applied Sciences 7 (1) (2017), https://doi.org/10.3390/app7010049.

[32] V. Madurai Ramakrishnan, M. N., B. P., S. Pitchaiya, D. Velauthapillai, A. Pugazhendhi, Transformation of TiO2 nanoparticles to nanotubes by simple solvothermal route and its performance as dye-sensitized solar cell (DSSC) photoanode, Int. J. Hydrogen Energy 45 (31) (2020) 15441–15452, https://doi.org/10.1016/j.ijhydene.2020.04.021.

[33] R.S. Dubey, K.V. Krishnamurthy, S. Singh, Experimental studies of TiO2 nanoparticles synthesized by sol-gel and solvothermal routes for DSSCs application, Results Phys. 14 (2019) 102390, https://doi.org/10.1016/j.rinp.2019.102390.

[34] J.C. Araújo, P. Teixeira, R. Fangueiro, D.P. Ferreira, Multifunctional natural fibers: the potential of core shell MgO–SiO2 nanoparticles, Cellulose (2022) 1–18.

[35] B. Lazić, et al., Influence of hemicelluloses and lignin content on structure and sorption properties of flax fibers (Linum usitatissimum L.), Cellulose 25 (2018), https://doi.org/10.1007/s10570-017-1575-4.

[36] D.P. Ferreira, A. Ferreira, R. Fangueiro, Searching for natural conductive fibrous structures via a green sustainable approach based on jute fibers and silver nanoparticles, Polymers (Basel). 10 (63) (2018), https://doi.org/10.3390/polym10010063.

[37] E. Portella, D. Romanzini, C. Angrizani, S. Amico, A. Zattera, Influence of stacking sequence on the mechanical and dynamic mechanical properties of cotton/glass Fiber reinforced polyester composites, Mater. Res. 19 (2016), https://doi.org/10.1590/1980-5373-MR-2016-0058.

[38] S. Khan, et al., Effect of particle size on the photocatalytic activity and sensing properties of CeO2 nanoparticles, Int. J. Electrochem. Sci. 8 (2013) 7284–7297.

[39] M. Culica, C.-S. Andreea, V. Melinte, S. Coseri, Cellulose acetate incorporating organically functionalized CeO2 NPs: efficient materials for UV filtering applications, Materials (Basel) 13 (2020) 2955, https://doi.org/10.3390/ma13132955.

[40] A.S. Ribeiro, S. Costa, D.P. Ferreira, A. Houcine, R. Fangueiro, Development of chitosan-gelatin nanofibers with cellulose nanocrystals for skin protection applications, Key Eng. Mater. 893 (2021) 45–55.

[41] S. Costa, D.P. Ferreira, P. Teixeira, L. Ballesteros, J. Teixeira, R. Fangueiro, Active natural-based films for food packaging applications: the combined effect of chitosan and nanocellulose, Int. J. Biol. Macromol. 177 (2021), https://doi.org/10.1016/j.ijbiomac.2021.02.105.

[42] D.M. Ridolfi, A.P. Lemes, S. de Oliveira, G.Z. Justo, M.V. Palladino, N. Durán, Electrospun poly(ethylene oxide)/chitosan nanofibers with cellulose nanocrystals as support for cell culture of 3T3 fibroblasts, Cellulose 24 (8) (2017) 3353–3365, https://doi.org/10.1007/s10570-017-1362-2.

[43] M. Pakravan, M.-C. Heuzey, A. Ajji, Core-shell structured PEO-chitosan nanofibers by coaxial electrospinning, Biomacromolecules 13 (2) (2012) 412–421, https://doi.org/10.1021/bm201444v.

[44] A. Al-Sabagh, M.E. Hassan, S. Dessouky, N. Nasser, E. El-sharaky, M. Mahmoud, Preparation of some thermal stable polymers based on diesters of polyethylene and polypropylene oxides macro monomers to use as surfactants at high temperature and pressure, Egypt. J. Pet. 25 (2015), https://doi.org/10.1016/j.ejpe.2015.08.001.

[45] S. Kuriechen, S. Murugesan, S. Raj, Mineralization of azo dye using combined photo-Fenton and photocatalytic processes under visible light, J. Catal. 2013 (2013), https://doi.org/10.1155/2013/104019. , Jan.

[46] G. Kandregula, D. Chinthakuntla, K. Rao, C. Chakra, V. Rajendar, Green Synthesis of TiO 2 Nanoparticles Using Hibiscus Flower Extract, 2014.

[47] K. Huang, L. Chen, L. Meixiang, J. Xiong, The photocatalytic inactivation effect of Fe-doped TiO2 nanocomposites on leukemic HL60 cells-based photodynamic therapy, Int. J. Photoenergy 2012 (2012), https://doi.org/10.1155/2012/367072.

[48] I. Nurhasanah, W. Safitri, Z. Arifin, A. Subagio, T. Windarti, Antioxidant activity and dose enhancement factor of CeO 2 nanoparticles synthesized by precipitation method, IOP Conf. Ser. Mater. Sci. Eng. 432 (2018) 12031, https://doi.org/10.1088/1757-899X/432/1/012031.

[49] S.S. Anesh, A. Mohamed, K. Mohan, A. Solaiappan, Enhanced near-infrared reflectance and functional characteristics of Al-doped ZnO nano-pigments

embedded PMMA coatings, Sol. Energy Mater. Sol. Cells 143 (2015) 335–346, https://doi.org/10.1016/j.solmat.2015.07.012.
[50] B. Pant, M. Park, S.-J. Park, Recent advances in TiO2 films prepared by sol-gel methods for photocatalytic degradation of organic pollutants and antibacterial activities, Coatings 9 (10) (2019), https://doi.org/10.3390/coatings9100613.
[51] K.S. Khashan, et al., Antibacterial activity of TiO2 nanoparticles prepared by one-step laser ablation in liquid, Appl. Sci. 11 (10) (2021), https://doi.org/10.3390/app11104623.
[52] T. Verdier, M. Coutand, A. Bertron, C. Roques, Antibacterial activity of TiO2 Photocatalyst alone or in coatings on E. Coli: the influence of methodological aspects, Coatings 4 (3) (2014) 670–686, https://doi.org/10.3390/coatings4030670.
[53] T.N. Ravishankar, T. Ramakrishnappa, G. Nagaraju, H. Rajanaika, Synthesis and characterization of CeO2 nanoparticles via solution combustion method for photocatalytic and antibacterial activity studies, ChemistryOpen 4 (2) (2015) 146–154, https://doi.org/10.1002/open.201402046.
[54] S. Lan, X. Sheng, Y. Lu, C. Li, S. Zhao, N. Liu, Modification of antibacterial ZnO nanorods with CeO2 nanoparticles: role of CeO2 in impacting morphology and antibacterial activity, Colloid Interface Sci. Commun. 26 (2018) 32–38, https://doi.org/10.1016/j.colcom.2018.08.002.
[55] A. Azam, A.S. Ahmed, M. Oves, M.S. Khan, S.S. Habib, A. Memic, Antimicrobial activity of metal oxide nanoparticles against gram-positive and gram-negative bacteria: a comparative study, Int. J. Nanomedicine 7 (2012) 6003–6009, https://doi.org/10.2147/IJN.S35347.
[56] V. Stanić, S.B. Tanasković, Chapter 11 - antibacterial activity of metal oxide nanoparticles, in: S. Rajendran, A. Mukherjee, T.A. Nguyen, C. Godugu, R.K.B.T.-N. Shukla (Eds.), Micro and Nano Technologies, Elsevier, 2020, pp. 241–274.
[57] Y.D. Cai, S. Bin Ma, Progress in the study of antibacterial fibers, Adv. Mater. Res. 821–822 (2013) 103–106, https://doi.org/10.4028/www.scientific.net/AMR.821-822.103.
[58] M. Ilangovan, V. Guna, C. Hu, G.S. Nagananda, N. Reddy, *Curcuma longa* L. plant residue as a source for natural cellulose fibers with antimicrobial activity, Ind. Crops Prod. 112 (September) (2018) 556–560, https://doi.org/10.1016/j.indcrop.2017.12.042.
[59] J.C. Araújo, D.P. Ferreira, P. Teixeira, R. Fangueiro, In-situ synthesis of CaO and SiO2 nanoparticles onto jute fabrics: exploring the multifunctionality, Cellulose (2020), https://doi.org/10.1007/s10570-020-03564-1.
[60] V.-P. Dinh, et al., Insight into the adsorption mechanisms of methylene blue and chromium(iii) from aqueous solution onto pomelo fruit peel, RSC Adv. 9 (44) (2019) 25847–25860, https://doi.org/10.1039/C9RA04296B.
[61] X.-H. Qin, S.-Y. Wang, Electrospun nanofibers from crosslinked poly(vinyl alcohol) and its filtration efficiency, J. Appl. Polym. Sci. 109 (2) (2008) 951–956, https://doi.org/10.1002/app.28003.
[62] U. Mahanta, M. Khandelwal, A.S. Deshpande, TiO2@SiO2 nanoparticles for methylene blue removal and photocatalytic degradation under natural sunlight and low-power UV light, Appl. Surf. Sci. 576 (2022) 151745, https://doi.org/10.1016/j.apsusc.2021.151745.
[63] S.M. Tichapondwa, J.P. Newman, O. Kubheka, Effect of TiO2 phase on the photocatalytic degradation of methylene blue dye, Phys. Chem. Earth, Parts A/B/C 118–119 (2020) 102900, https://doi.org/10.1016/j.pce.2020.102900.
[64] K. Al-hamoud, et al., Pulicaria undulata extract-mediated eco-friendly preparation of TiO2 nanoparticles for photocatalytic degradation of methylene blue and methyl Orange, ACS Omega 7 (6) (2022) 4812–4820, https://doi.org/10.1021/acsomega.1c05090.
[65] S. Krishnan, A. Shriwastav, Application of TiO2 nanoparticles sensitized with natural chlorophyll pigments as catalyst for visible light photocatalytic degradation of methylene blue, J. Environ. Chem. Eng. 9 (1) (2021) 104699, https://doi.org/10.1016/j.jece.2020.104699.
[66] A. Raees, M.A. Jamal, I. Ahmed, M. Silanpaa, T. Saad Algarni, Synthesis and characterization of CeO2/CuO nanocomposites for photocatalytic degradation of methylene blue in visible light, Coatings 11 (3) (2021), https://doi.org/10.3390/coatings11030305.
[67] M.A. Zeleke, D.-H. Kuo, Synthesis and application of V2O5-CeO2 nanocomposite catalyst for enhanced degradation of methylene blue under visible light illumination, Chemosphere 235 (2019) 935–944, https://doi.org/10.1016/j.chemosphere.2019.06.230.
[68] D. Majumder, I. Chakraborty, K. Mandal, S. Roy, Facet-dependent Photodegradation of methylene blue using pristine CeO2 nanostructures, ACS Omega 4 (2) (2019) 4243–4251, https://doi.org/10.1021/acsomega.8b03298.
[69] J.C. Cano-Franco, M. Álvarez-Láinez, Effect of CeO2 content in morphology and optoelectronic properties of TiO2-CeO2 nanoparticles in visible light organic degradation, Mater. Sci. Semicond. Process. 90 (2019) 190–197, https://doi.org/10.1016/j.mssp.2018.10.017.
[70] F. Chen, et al., Synergistic effect of CeO2 modified TiO2 photocatalyst on the enhancement of visible light photocatalytic performance, J. Alloys Compd. 714 (2017) 560–566, https://doi.org/10.1016/j.jallcom.2017.04.138.
[71] J. Tian, et al., Enhanced photocatalytic performances of CeO2/TiO2 nanobelt heterostructures, Small 9 (22) (2013) 3864–3872, https://doi.org/10.1002/smll.201202346.
[72] D.A. Panayotov, J.R. Morris, Uptake of a chemical warfare agent simulant (DMMP) on TiO2: reactive adsorption and active site poisoning, Langmuir 25 (6) (2009) 3652–3658.
[73] G.W. Wagner, et al., Reactions of VX, GB, GD, and HD with nanosize Al2O3. Formation of aluminophosphonates, J. Am. Chem. Soc. 123 (8) (2001) 1636–1644.
[74] G.W. Wagner, P.W. Bartram, O. Koper, K.J. Klabunde, Reactions of VX, GD, and HD with nanosize MgO, J. Phys. Chem. B 103 (16) (1999) 3225–3228.
[75] A.R. Wilmsmeyer, et al., Infrared spectra and binding energies of chemical warfare nerve agent simulants on the surface of amorphous silica, J. Phys. Chem. C 117 (30) (2013) 15685–15697.
[76] P. Makie, G. Westin, P. Persson, L. Osterlund, Adsorption of trimethyl phosphate on maghemite, hematite, and goethite nanoparticles, J. Phys. Chem. A 115 (32) (2011) 8948–8959.
[77] W.C. Hung, J.C. Wang, K.H. Wu, Adsorption and decomposition of dimethyl methylphosphonate (DMMP) on expanded graphite/metal oxides, Appl. Surf. Sci. 444 (2018) 330–335, https://doi.org/10.1016/j.apsusc.2018.03.082.
[78] S. Mukhopadhyay, M. Schoenitz, E.L. Dreizin, Vapor-phase decomposition of dimethyl methylphosphonate (DMMP), a sarin surrogate, in presence of metal oxides, Def. Technol. 17 (4) (2021) 1095–1114, https://doi.org/10.1016/j.dt.2020.08.010.
[79] S. Holdren, et al., Adsorption and destruction of the G-series nerve agent simulant dimethyl methylphosphonate on zinc oxide, ACS Catal. 9 (2) (2018) 902–911.